2019 IEEE Symposium Series on Computational Intelligence (SSCI)
December 6-9 2019, Xiamen, China

A Novel Assist-As-Needed Controller Based on Fuzzy-Logic Inference and Human Impedance Identification for Upper-Limb Rehabilitation

Chen Wang, Liang Peng, Zeng-Guang Hou, and Weiqun Wang
State Key Laboratory of Management and Control
for Complex Systems, Institute of Automation,
Chinese Academy of Sciences, Beijing 100190, China
Emails: {wangchen2016, liang.peng, zengguang.hou, weiqun.wang}@ia.ac.cn

Tingting Su
Department of Mechanical and Electrical
Engineering, North China University
of Technology, Beijing, 100144, P.R. China
Email: sutingting@ncut.edu.cn

***Abstract*—Upper-limb rehabilitation robots are being increasingly included in the rehabilitation after stroke. Clinical studies suggest that the patient's active participation can maximize effectiveness of robot-assisted rehabilitation and result in fastest possible recovery. In order to promote active involvement of the patient, we develop a subject-adaptive controller within the assist-as-needed (AAN) paradigm. The controller employs Recursive Least Square (RLS) algorithm to identify human arm impedance parameters, with aims to quantify the residual motor capability of the patient. According to the upper-limb impedance of the patient in the direction along movements, the reference trajectory can be generated based on the motion patterns in healthy humans. In addition, the fuzzy logic control strategy is implemented in the direction perpendicular to movements, which is capable of adjusting the robotic assistance level by considering both upper-limb impedance of the patient and the variations of deviation between the reference trajectory and actual trajectory. Furthermore, the proposed subject-adaptive AAN controller was validated in the simulation study, and the results demonstrated the capability of the controller to modulate the assistance level in accordance with the subject's instantaneous requirements. Future works will focus on the implementation of the control scheme with post-stroke patients.**

Keywords*—*Assist-as-needed; fuzzy logic control; rehabilitation robotics; identification of human arm impedance.

I. Introduction

Stroke is induced by intracerebral haemorrhage or infarction, and is one of the main causes of non-traumatic disability in humans [1]. According to statistical results from WHO (World Health Organization), the absolute numbers of people suffering from stroke annually exceed 15 million [2]. Most post-stroke patients are left with severe upper-limb motor disability, which affect the performances in ADLs (activities of daily living) [3]. In order to help these patients restore the lost motor functions, long-term and high-intensity rehabilitation (i.e., physical therapy and occupational therapy) are considered essential. Compared with the traditional therapy accomplished manually by therapists, robot-assisted rehabilitation is well suited for rehabilitation training for the advantages in consistent delivery of therapy, objective and quantitative assessment, virtual reality interfaces, etc [4].

The effectiveness of robot-aided rehabilitation relies heavily on control strategies, and the existing robotic therapy strategies can be roughly divided into passive training and active training. Hogan et al. [5] demonstrated that passive trajectory tracking did not effectively promote the motor recovery in stroke survivors, suggesting that active participation plays an important role in motor relearning. Furthermore, there are evidences that high-level active participation can induce neural plasticity and hence result in fastest possible recovery [6]. In order to maximize patients' active participation, the assist-as-needed (AAN) control paradigm [7] has been proposed, with aims to minimize robotic assistance based on patients' online performance.

The implementation of AAN control, however, remains an open-ended research area. By considering that excessive assistance tends to increase the patient's slackness and insufficient assistance may lead to patient's depression, it is critical to determine the optimal assistance that rehabilitation robots should provide. Previous studies used electroencephalography (EEG) and electromyography (EMG) signals to predict human intended motion in rehabilitation robotic systems [8], [9]. These methods have limitations in decoding motion commands with high precision because the state-of-the-art pattern recognition techniques are limited in separating certain types of predefined motions. Wolbrecht et al. [10] first utilized Gaussian radial basis functions (RBFs) to model the motor functional status of the patient, for the purposes of AAN rehabilitation. Pehlivan et al. [11] similarly integrated directionally dependent RBFs with adaptive control law to provide assistance only when the patient has insufficient motor ability. A drawback of such approaches is that the fixed error bounds can not simultaneously satisfy the variable performance of post-stroke patients during training tasks.

Addressing the above problems, the effectiveness of robot-

This work was supported in part by National Natural Science Foundation of China (Grant #61720106012, 61603386, 61421004, U1613228, 61533016) and Beijing Natural Science Foundation (Grant L172050), and also supported by the Strategic Priority Research Program of Chinese Academy of Science (Grant No.XDB32040000).

978-1-7281-2485-8/19/$31.00 ©2019 IEEE

assisted rehabilitation can be augmented by developing a controller capable of faithfully reacting to temporal variabilities in patients' performance and optimizing the human-robot interaction. By considering that the dynamics of coupled human-robot system are complicated and changeable during the rehabilitation training, the formulation of a subject-adaptive AAN controller consists of two vital tasks. The first task is to generate the reference trajectory online according to the residual motor capability of the patient, furthermore, the common patterns of movements in healthy humans should be emphasized. Then the robot provides the patient with only necessary assistance by estimating the patient's active effort. To accomplish the above tasks, fuzzy logic control is suitable to be integrated into the controller due to the capability of unknown disturbances compensation. Many researches have implemented fuzzy-based controllers in passive rehabilitation training [12], [13], therefore, there is considerable interest in the development of an subject-adaptive AAN controller based on fuzzy-logic inference.

In this study, we propose a novel subject-adaptive AAN controller, which utilizes Recursive Least Square (RLS) algorithm to identify human arm impedance parameters and reflect the movement intention, and then implement fuzzy-logic inference to adjust the robotic assistance according to patients' instantaneous requirements in a timely manner. There are two parts in the AAN control framework: in the advancing direction, the optimal reference trajectory is generated by integrating the upper-limb stiffness and minimum-jerk model [14], which focuses on the patient's instantaneous performance and the motion patterns in healthy humans, and then impedance control is applied to achieve online trajectory tracking; in the perpendicular direction, the fuzzy logic control strategy is used to optimize the robotic assistance by considering both the variations of deviation errors and upper-limb impedance, with the aim to adaptively maximize patients' active participation.

This paper is organized as follows. Section II describes the upper-limb rehabilitation robot and details the robot mechanism design. Section III presents the subject-adaptive AAN controller consisting of three novel parts, and the proposed controller is validated in Section IV. Then the simulation results are presented in Section V, and Section VI concludes the study.

II. Upper-Limb Rehabilitation Robot Description

We have developed an upper-limb rehabilitation robot, which adopts the end-effector based structure (see Fig. 1). A five-bar parallel mechanism is formed by five revolute joints and four links, where two base joints are coaxial and actuated by DC motors, respectively. By combining a highly backdrivable belt transmission, the robot has a compact structure and is easy to maintain. The details of technical specifications are shown in Table I .

In the the rehabilitation training, patients are seated in a high back chair with hips and knees flexed 90°, and couple their affected arm with the end-effector of the robot. As the robot is capable of assisting shoulder and elbow joints, patients can complete 2 degree-of-freedom (DOF) movements with the residual motor capability. Further, a virtual reality environment is developed to best promote the patient's motivation.

Fig. 1: The upper-limb rehabilitation robot.

TABLE I: Technical Specifications

Items	Characteristics
DOF	2
Actuation	2 DC motors
Sensors	2 rotary encoders
Range of Joint Motion	-20°∼80°, 80°∼190°
Workspace	600 mm * 450 mm

III. Fuzzy-Based Framework for AAN Control

In this section, we present the subject-adaptive AAN controller, which employs RLS algorithm to identify human arm impedance parameters, and then utilizes fuzzy logic algorithm to develop the AAN controller in the perpendicular direction. Fig. 2 shows the key blocks of the proposed controller, including the identification of human arm impedance, reference trajectory planning, and controller regulation based on fuzzy-logic inference. The framework of the fuzzy-based AAN controller can be described as the three main aspects:

- As the reaching capability is considered as the basis for most ADLs, this study focuses on the reaching tasks along the Y axis. Based on the human-robot interaction force and the robot end-effector position, the upper-limb impedance parameters can be identified by RLS algorithm, which reflects the instantaneous performance and requirements of the subject.
- In the advancing direction, the real-time trajectory generation scheme is implemented based on the upper-limb stiffness and minimum-jerk principle, which concentrates on both the subjects movement intention and human normal motion patterns. In addition, a feedback impedance controller is developed to regulate the tracking error.
- In the perpendicular direction, the upper-limb impedance and the variations of deviation between the actual trajectory and reference trajectory are served as the inputs of a fuzzy-based controller, which is capable of maximizing active involvement of the subject.

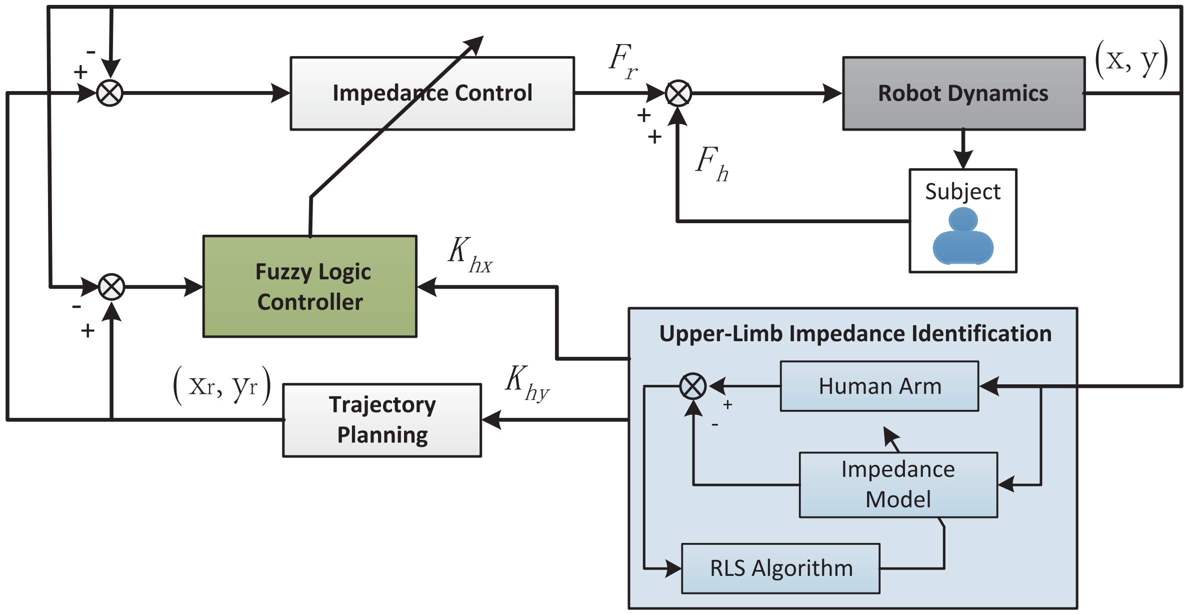

Fig. 2: Overview of the subject-adaptive AAN control. The key parts of the control scheme consist of the identification of human arm impedance, trajectory planning in the advancing direction, and fuzzy logic control in the perpendicular direction.

The following subsections introduce the details of these key methods.

A. Identification of Upper-Limb Impedance

The dynamic behavior of human movements can be described by the mechanical impedance (i.e., stiffness, damping and inertia) [15]. This study estimates the impedance characteristics of upper extremity in order to delineate the residual motor capability of the patient. To begin with, the human upper-limb dynamics can be expressed in the form of spring-damp impedance model:

$$F_h = K_h \Delta X + B_h \Delta \dot{X}, \tag{1}$$

where F_h is the human-robot interaction force, $X = [x, y]^T$ is displacement of the arm, and K_h, B_h are stiffness and damping matrices, which defined respectively by:

$$K_h = \begin{bmatrix} K_{hx} & 0 \\ 0 & K_{hy} \end{bmatrix}, B_h = \begin{bmatrix} B_{hx} & 0 \\ 0 & B_{hy} \end{bmatrix}.$$

In order to simplify the estimation of the unknown impedance parameters, the model can be rearranged into a linear form with respect to θ as below:

$$\Phi \theta = F_h, \tag{2}$$

where

$$\Phi = \begin{bmatrix} \Delta x & \Delta \dot{x} & 0 & 0 \\ 0 & 0 & \Delta y & \Delta \dot{y} \end{bmatrix}$$

$$\theta = \begin{bmatrix} K_x & B_x & K_y & B_y \end{bmatrix}^T.$$

The impedance parameters can be estimated by discrete-time adaptive identification method, and Fig. 2 illustrates the parameter estimation system. According to the RLS algorithm [16], the process of parameter adjustment can be described by the following formulas:

$$R(k) = \frac{Q(k-1)\phi(k-1)}{\lambda + \phi^T(k-1)Q(k-1)\phi(k-1)} \tag{3}$$

$$Q(k) = \frac{(Q(k-1) - R(k)\phi^T(k-1)Q(k-1))}{\lambda} \tag{4}$$

$$\begin{aligned}\hat{\theta}(k) = \hat{\theta}(k-1) + \\ R(k)(F_h(k) - \phi^T(k-1)\hat{\theta}(k-1))\end{aligned} \tag{5}$$

where $\hat{\theta}(k)$ denotes the vector containing the unknown parameters, with k the number of sampling points; $R(k)$ and $Q(k)$ are covariance matrix and gain vector, respectively; $0 < \lambda \leq 1$ is the forgetting factor.

B. Trajectory Planning in the Advancing Direction

Point-to-point reaching movements are the most commonly used training task in upper-limb rehabilitation after stroke. Numerous observations have demonstrated that unconstrained point-to-point reaching movements in healthy humans have similar characteristics, and the minimum-jerk model is most prominent among these invariant characteristics [14]. In essence, this model aims to maximize the smoothness of the reaching movements, which can be expressed as the minimization of a cost function C:

$$C = \frac{1}{2} \int_{t_1}^{t_2} \left[\left(\frac{d^3x}{dt^3} \right)^2 + \left(\frac{d^3y}{dt^3} \right)^2 \right] dt, \tag{6}$$

where (x, y) is the end-effector position's Cartesian coordinates.

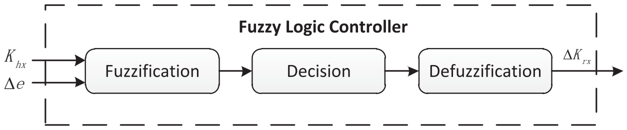

Fig. 3: Fuzzy logic controller deployed into the system.

Therefore, the actual trajectory between (x_i, y_i) and (x_d, y_d) can be simplified to:

$$\begin{aligned} &\tfrac{x(t)-x_i}{x_d-x_i} = \tfrac{y(t)-y_i}{y_d-y_i} \\ &= 10(t/T_d)^3 - 15(t/T_d)^4 + 6(t/T_d)^5 \end{aligned}, \tag{7}$$

where T_d denotes the total movement time. It can be verified that the minimum-jerk trajectory is a straight line connecting the two points with a bell-shaped speed profile.

For repetitive point-to-point reaching movements along the Y axis, the reference trajectory from (x_i, y_i) to (x_d, y_d) is simplified as:

$$\begin{aligned} &x_r = 0 \\ &y_r = y_i + (y_d - y_i)\left[10(\tfrac{t}{T_d})^3 - 15(\tfrac{t}{T_d})^4 + 6(\tfrac{t}{T_d})^5\right]. \end{aligned} \tag{8}$$

For the time being assume that the starting point and ending point are defined beforehand, the optimal reference trajectory can be determined by the movement time T_d. As the impedance characteristics are capable of reflecting the human movement intention, T_d is adjusted according to the stiffness parameters of the subject in the advancing direction:

$$T_d(t) = T_d(t-1) - \gamma\left(K_{hy}(t) - K_{hy}(t-1)\right), \tag{9}$$

where γ is an adjustment factor, and the increase of human stiffness K_{hy} causes the decrease of T_d.

The above reference trajectory is synchronous with the real-time performance of the subject, and also compliant with the motion patterns in healthy humans. Consequently, the robot tends to decrease the training velocity for the more impaired subject, and presents greater challenges for the less impaired subject.

C. Fuzzy Logic Control in the Perpendicular Direction

The fuzzy logic controller has been developed to make decisions on adjusting the robotic assistance according to the temporal variabilities in patients' performance and requirements. As shown in Fig. 3, the proposed controller has a multi-input single-output (MISO) structure based on the Mamdani fuzzy model [17].

The impedance controller used in the workspace can be mathematically expressed as:

$$\begin{aligned} &F_{rx}(t) = -K_{rx}x(t) - B_{rx}\dot{x}(t) \\ &F_{ry}(t) = K_{ry}(y_r(t) - y(t)) + B_{ry}(\dot{y}_r(t) - \dot{y}(t)) \\ &\tau_r(t) = J^T[F_{rx}(t), F_{ry}(t)]^T \end{aligned} \tag{10}$$

where (K_{rx}, K_{ry}) is robot stiffness parameters in the x and y directions, and (B_{rx}, B_{ry}) is the robot damping factors in the x and y directions.

TABLE II: Fuzzy Rules Of ΔK_{rx}

K_{hx} \ Δe	**NB**	**NS**	**ZE**	**PS**	**PB**
NB	NS	ZE	ZE	PS	PB
NS	NS	ZE	ZE	PS	PS
ZE	NS	NS	ZE	PS	PS
PS	NB	NS	ZE	ZE	PS
PB	NB	NB	ZE	ZE	PS

The robot stiffness parameters in the x direction is adjusted by the fuzzy logic controller based on two inputs: the variations of deviation errors (Δe) and the upper-limb stiffness (K_{hx}). For fuzzification, triangular and trapezoidal membership functions are used for the inputs and output, and the linguistic terms include Big Negative (NB), Small Negative (NS), Zero (ZE), Small Positive (PS) and Big Positive (PB). Then the fuzzy IF-THEN rules are defined to determine the relationship between Δe, K_{hx}, and ΔK_{rx}, as illustrated in Table II. For the defuzzification operation, center-of-area method (COA) is employed, which can be expressed as:

$$z^* = \frac{\int_y z\mu_B(z)dz}{\int_y \mu_B(z)dz}, \tag{11}$$

where z is the output of the fuzzy logic controller, and z^* denotes the true value of the output; B is a fuzzy set, and $\mu_B(z)$ represents the membership degrees of B at z.

Consequently, the amount of robotic assistance can be increased (i.e., a larger K_{rx}) when the patient's performance exacerbates the deviation error, which means that the patient can hardly complete the reference trajectory by his/her own ability. Conversely, once the patient demonstrates some degrees of self-adjustment ability, the robot would decrease the assistance level with the aim to let the patient explore upper extremity motor control.

IV. Simulation

The developed subject-adaptive AAN controller was validated by simulation in MATLAB (MathWorks Inc.). In order to demonstrate the capability of the controller to optimize the assistance force according to the subject's performance, the various conditions of human arm impedance was investigated in the simulation study.

To begin with, we simplified the upper-limb rehabilitation robot as a five-bar parallel mechanism (see Fig. 4). The coordinates of the end-effector $P(x, y)$ can be expressed as:

$$\begin{bmatrix} x \\ y \end{bmatrix} = \begin{bmatrix} l_2\cos q_2 + l_3\cos q_1 \\ l_2\sin q_2 + l_3\sin q_1 \end{bmatrix}, \tag{12}$$

The linear velocity of P is

$$\begin{bmatrix} \dot{x} \\ \dot{y} \end{bmatrix} = \begin{bmatrix} -l_3\sin q_1 & -l_2\sin q_2 \\ l_3\cos q_1 & l_2\cos q_2 \end{bmatrix}\dot{q}, \tag{13}$$

where $q = \begin{bmatrix} q_1 & q_2 \end{bmatrix}^T$.

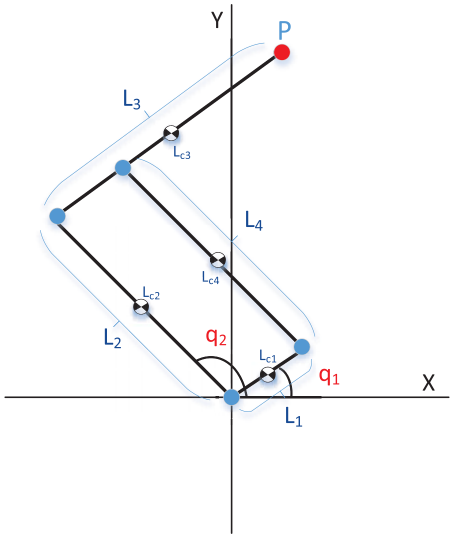

Fig. 4: Structure of the robot mechanism design.

Then the velocity Jacobian can be derived as:

$$J = \begin{bmatrix} -l_3 \sin q_1 & -l_2 \sin q_2 \\ l_3 \cos q_1 & l_2 \cos q_2 \end{bmatrix}. \tag{14}$$

By applying Lagrange-based dynamics modeling procedure, we can obtain the the inertia matrix D:

$$D = \begin{bmatrix} d_{11}(q) & d_{12}(q) \\ d_{21}(q) & d_{22}(q) \end{bmatrix}, \tag{15}$$

where

$$d_{11}(q) = m_1 l_{c1}^2 + m_3 l_{c3}^2 + m_4 l_1^2 + I_1 + I_3$$
$$d_{12}(q) = d_{21}(q) = (m_3 l_2 l_{c3} + m_4 l_1 l_{c4}) \cos(q_2 - q_1)$$
$$d_{22}(q) = m_2 l_{c2}^2 + m_3 l_2^2 + m_4 l_{c4}^2 + I_2 + I_4.$$

In this case the centripetal and Coriolis matrix C is given as:

$$C = \begin{bmatrix} 0 & h\dot{q}_2 \\ -h\dot{q}_1 & 0 \end{bmatrix}, \tag{16}$$

where

$$h = -(m_3 l_2 l_{c3} + m_4 l_1 l_{c4}) \sin(q_2 - q_1).$$

Hence, the dynamic equations of the robot can be expressed in the following form:

$$D(q)\ddot{q} + C(q, \dot{q})\dot{q} = \tau. \tag{17}$$

As the upper-limb impedance is defined at the interaction port in the workspace, its more convenient to transform the above dynamic model into the workspace form:

$$\hat{D}\ddot{X} + \hat{C}\dot{X} = F_r + F_h, \tag{18}$$

where

$$\begin{matrix} \hat{D} = J^{-T} D J^{-1} \\ \hat{C} = J^{-T}(-DJ^{-1}\dot{J} + C)J^{-1} \end{matrix},$$

and $X = [x, y]^T$ is the end-effector position, $F_r = J^{-T}\tau$ and F_h represent the robotic equivalent force and human active force at the endpoint. The mathematical calculations used to derive the robot dynamics can be found in our previous work [18].

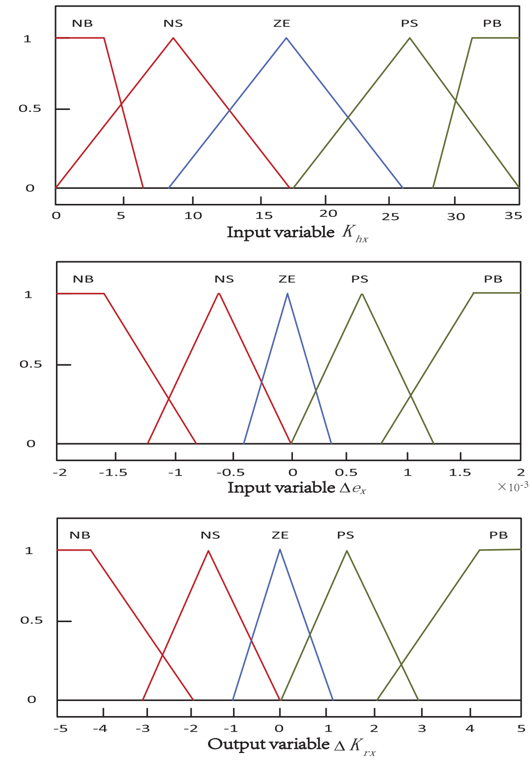

Fig. 5: The membership functions of K_{hx}, Δe_x and ΔK_{rx}, the units are N/m, mm and N/m respectively.

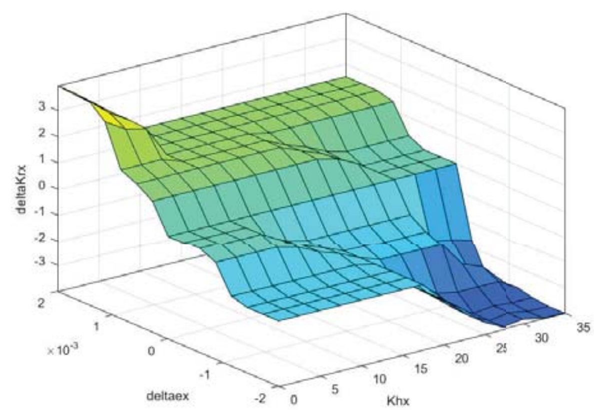

Fig. 6: Surface viewer of the fuzzy inference system.

Based on the system dynamics (18), we implemented the proposed controller in the point-to-point reaching movements along the Y axis. Specifically, the membership functions of the fuzzy logic controller are shown in Fig. 5, and the surface viewer of the fuzzy logic inference system is presented in Fig. 6.

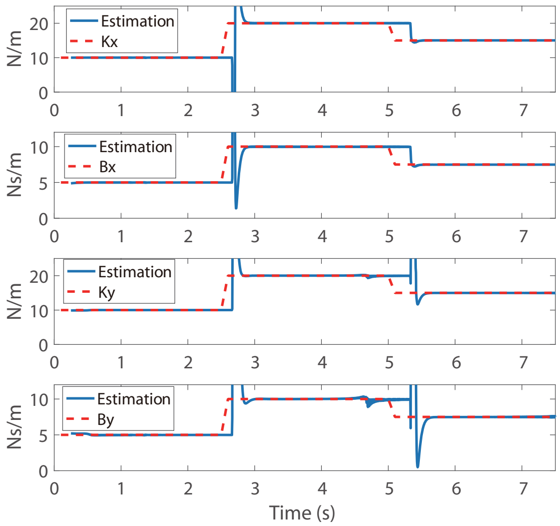

Fig. 7: The identification results of upper-limb impedance by utilizing RLS algorithm

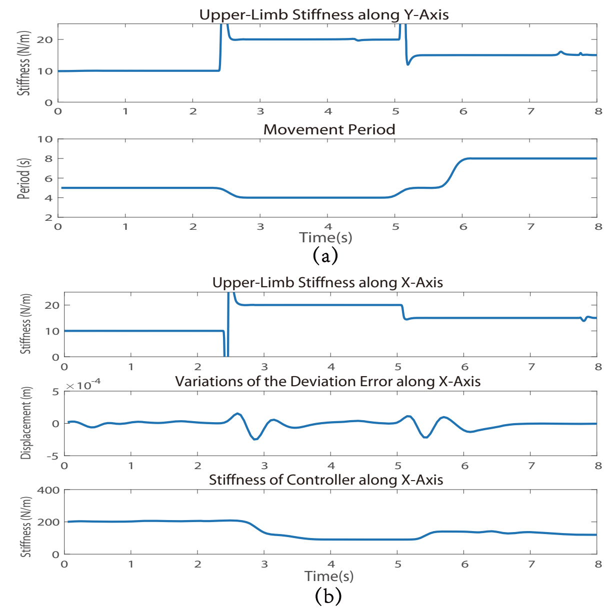

Fig. 8: Results from the subject-adaptive AAN controller. (a) Illustration of the trajectory planning in the direction along the movements, where the movement period varies with the upper-limb stiffness. (b) Illustration of the fuzzy-based controller in the direction perpendicular to the movements, where the controller stiffness changes with the upper-limb stiffness and the variations of deviation errors.

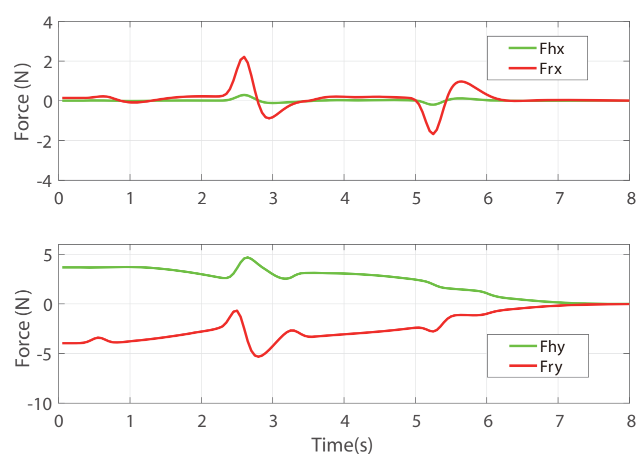

Fig. 9: Robotic assistance force F_h and human active force F_r in the directions perpendicular and advancing to the movements.

V. Results

In this section, we present the results from the aforementioned simulation, and further analyze the performance of human arm impedance identification, trajectory planning in the advancing direction, and fuzzy logic inference in the perpendicular direction.

In order to validate the adaptation performance of the subject-adaptive AAN controller, the upper-limb impedance was set to abruptly increase at 2.5 seconds, and then reduce at 5 seconds. The results of human impedance identification employing RLS algorithm is shown in Fig. 7, where we can see that the estimated impedance complied well with the actual values.

Considering the training task was the reaching movements along the Y axis, the reference trajectory was generated according to the identification results and minimum-jerk model (see Fig. 8(a)). The movement period was adjusted according to the upper-limb stiffness, and a larger stiffness value reflected the increase of motion motivation, thus the desired motion time was shortened and the trajectory is regenerated online.

Once the reference trajectory was determined, the fuzzy-based controller modulated the robot stiffness by integrating the identification results and the variations of deviation errors (see Fig. 8(b)). In the perpendicular direction, the increase of upper-limb stiffness means that the subject has a better self-adjustment ability, hence the robotic assistance can be gradually reduced to some extent based on the deviation between the actual trajectory and reference trajectory.

Furthermore, a comparison between the force imposed by the subject and the robot is shown in Fig. 9. It can be seen that the robot is capable of providing compliant human-robot interaction to assist the subject to complete the training task. For instance, when the subject has difficulty in completing the desired movements, the robotic assistance level can be adaptively adjusted by decreasing the desired velocity in the advancing direction, and augmenting the controller stiffness based on fuzzy logic inference in the perpendicular direction; On the contrary, when the subject demonstrates proficiency, the requirement of the reference movements would be increased and the lower assistance level would be presented.

VI. Conclusion

This study presents a novel subject-adaptive AAN controller for upper-limb rehabilitation after stroke. The contribution of this control scheme is to optimize human-robot interaction online in the directions perpendicular and advancing to the movements. In order to faithfully delineate the residual motor capability of the patient, we employed RLS algorithm to identify human arm impedance parameters. Based on the identification results and minimum-jerk principle, the optimal reference trajectory was generated in the advancing direction, which can be synchronized with the subject's movement intention and compliant with the motion patterns in healthy humans. Furthermore, a fuzzy logic controller was developed in the perpendicular direction, which can adjust the robotic assistance level according to the upper-limb impedance and variations of deviation errors. As the fuzzy logic inference was capable of overcoming unknown disturbances, the proposed controller can adaptively ensure active participation of the patient, and thus complies well with the "assist-as-needed" principle.

The obtained results demonstrated the efficacy of developed subject-adaptive AAN controller, and validated the capability of the controller to optimize the assistance level according to the patient's instantaneous requirements. The future research will concentrate on demonstrating the control scheme experimentally with post-stroke patients in our upper-limb rehabilitation robot.

References

[1] V. L. Feigin, M. H. Forouzanfar, and R. Krishnamurthi, "Global and regional burden of stroke during 1990–2010: findings from the global burden of disease study 2010," *The Lancet*, vol. 383, no. 9913, pp. 245–255, 2014.

[2] N. Jackson, E. Haxton, and K. Morrison, "Reflections on 50 years of neuroscience nursing: the growth of stroke nursing," *Journal of Neuroscience Nursing*, vol. 50, no. 4, pp. 188–192, 2018.

[3] M. M. Ouellette, N. K. LeBrasseur, and J. F. Bean, "High-intensity resistance training improves muscle strength, self-reported function, and disability in long-term stroke survivors," *Stroke*, vol. 35, no. 6, pp. 1404–1409, 2004.

[4] A. C. Lo, P. D. Guarino, and L. G. Richards, "Robot-assisted therapy for long-term upper-limb impairment after stroke," *New England Journal of Medicine*, vol. 362, no. 19, pp. 1772–1783, 2010.

[5] N. Hogan, H. I. Krebs, and B. Rohrer, "Motions or muscles? some behavioral factors underlying robotic assistance of motor recovery." *Journal of Rehabilitation Research & Development*, vol. 43, no. 5, 2006.

[6] Z. Warraich and J. A. Kleim, "Neural plasticity: the biological substrate for neurorehabilitation," *PM&R*, vol. 2, no. 12, pp. S208–S219, 2010.

[7] L. Marchal-Crespo and D. J. Reinkensmeyer, "Review of control strategies for robotic movement training after neurologic injury," *Journal of neuroengineering and rehabilitation*, vol. 6, no. 1, p. 20, 2009.

[8] E. López-Larraz, L. Montesano, and Á. Gil-Agudo, "Continuous decoding of movement intention of upper limb self-initiated analytic movements from pre-movement eeg correlates," *Journal of neuroengineering and rehabilitation*, vol. 11, no. 1, p. 153, 2014.

[9] K. Veer and T. Sharma, "A novel feature extraction for robust emg pattern recognition," *Journal of medical engineering & technology*, vol. 40, no. 4, pp. 149–154, 2016.

[10] E. T. Wolbrecht, V. Chan, and D. J. Reinkensmeyer, "Optimizing compliant, model-based robotic assistance to promote neurorehabilitation," *IEEE Transactions on Neural Systems and Rehabilitation Engineering*, vol. 16, no. 3, pp. 286–297, 2008.

[11] A. U. Pehlivan, F. Sergi, and M. K. O'Malley, "A subject-adaptive controller for wrist robotic rehabilitation," *IEEE/ASME Transactions on Mechatronics*, vol. 20, no. 3, pp. 1338–1350, 2014.

[12] Z. Chen, Z. Li, and C. P. Chen, "Disturbance observer-based fuzzy control of uncertain mimo mechanical systems with input nonlinearities and its application to robotic exoskeleton," *IEEE transactions on cybernetics*, vol. 47, no. 4, pp. 984–994, 2016.

[13] A. Karime, M. Eid, and J. M. Alja'Am, "A fuzzy-based adaptive rehabilitation framework for home-based wrist training," *IEEE Transactions on Instrumentation and Measurement*, vol. 63, no. 1, pp. 135–144, 2013.

[14] T. Flash and N. Hogan, "The coordination of arm movements: an experimentally confirmed mathematical model," *Journal of neuroscience*, vol. 5, no. 7, pp. 1688–1703, 1985.

[15] F. A. Mussa-Ivaldi, N. Hogan, and E. Bizzi, "Neural, mechanical, and geometric factors subserving arm posture in humans," *Journal of Neuroscience*, vol. 5, no. 10, pp. 2732–2743, 1985.

[16] M. H. Hayes, "9.4: Recursive least squares," *Statistical Digital Signal Processing and Modeling*, p. 541, 1996.

[17] E. H. Mamdani and S. Assilian, "An experiment in linguistic synthesis with a fuzzy logic controller," *International journal of man-machine studies*, vol. 7, no. 1, pp. 1–13, 1975.

[18] C. Wang, L. Peng, and Z.-G. Hou, "Genetic algorithm based dynamics modeling and control of a parallel rehabilitation robot," in *Proceedings of IEEE International Conference on Evolutionary Computation (CEC)*, 2018, pp. 1–6.